

**Physica Status Solidi A: Applications and Materials Science**  
**Influence of Illumination Spectrum on Dissociation Kinetics of Iron-boron Pairs in Silicon**  
--Manuscript Draft--

<b>Manuscript Number:</b>	pssa.202400351R1
<b>Article Type:</b>	Research Article
<b>Corresponding Author:</b>	Oleg Olikh, Dr. Hab. Taras Shevchenko National University of Kyiv Kyiv, UKRAINE
<b>Corresponding Author E-Mail:</b>	olegolikh@knu.ua
<b>Order of Authors (with Contributor Roles):</b>	Oleg Olikh, Dr. Hab. (Conceptualization: Lead; Formal analysis: Lead; Investigation: Equal; Software: Lead; Validation: Equal; Visualization: Equal; Writing – original draft: Equal; Writing – review & editing: Equal)  Oleksandr Datsenko, PhD (Investigation: Equal; Validation: Equal; Writing – original draft: Equal; Writing – review & editing: Equal)  Serhiy Kondratenko, Dr. Hab. (Project administration: Equal; Resources: Lead; Writing – original draft: Equal; Writing – review & editing: Equal)
<b>Section/Category:</b>	(B) Gettering and Defect Engineering in Semiconductor Technology (GADEST 2024)
<b>Abstract:</b>	Photo-dissociation kinetics of iron–boron (FeB) pairs in boron-doped Czochralski silicon was studied experimentally using different light sources. It was shown that the FeB dissociation rate depends not only on integrated light intensity and overall carrier generation rate, but also on spectral composition of illumination. The value of the material constant of dissociation K varies and has been determined to be within (1.5–3.8) fs. The investigation has revealed an increase in the dissociation rate with increase in photon energy. The results indicate that recombination-enhanced defect reaction is the primary factor in the second stage of pair dissociation.
<b>Author Comments:</b>	
<b>Additional Information:</b>	
<b>Question</b>	<b>Response</b>
Please submit a plain text version of your cover letter here.	Dear Editors,  Enclosed with this letter you will find the electronic submission of manuscript entitled ``Influence of illumination spectrum on dissociation kinetic of iron-boron pairs in silicon'' by Oleg Olikh, Oleksandr Datsenko, and Serhiy Kondratenko.  It is widely recognized, that defects significantly impact semiconductor properties. Therefore it's crucial to understand the parameters of defects and the mechanisms behind their alteration, which holds significant practical importance. Over several decades, extensive knowledge has been amassed regarding specific defects, with the iron-boron pair in silicon being a well-studied example. Therefore, the discovery of new findings or the resolution of contentious issues is particularly intriguing.  It has been established that the rate of light-induced dissociation of FeB pairs is influenced by integrated illumination intensity, temperature, and the defect composition of the material. Our investigation found that the spectral composition of illumination is an additional important factor affecting dissociation efficiency. Specifically, we demonstrated that increased photon energy leads to higher photo-dissociation efficiency. The results indicate that the recombination-enhanced defect

	<p>reaction is the more probable mechanism at the second stage of light-induced dissociation, as opposed to iron ion recharge. We are confident that this study, shedding new light on the long-studied FeB pair in silicon, will be of significant interest to your readers.</p> <p>The corresponding abstract has been accepted for poster presentation at the 20th Conference on Gettering and Defect Engineering in Semiconductor Technology (GADEST 2024, Reference ID 105868).</p> <p>This is an original paper which has not been simultaneously submitted as a whole or in part anywhere else. No elements of the work have been published in any form. No conflict of interest exists in the submission of this manuscript.</p> <p>We would very much appreciate if you would consider the manuscript for publication in the GADEST 2024 special issue in <i>physica status solidi (a)</i>.</p> <p>Sincerely yours, Oleg Olikh and co-authors.</p> <p>Taras Shevchenko National University of Kyiv Kyiv 01601, Ukraine E-mail: <a href="mailto:olegolikh@knu.ua">olegolikh@knu.ua</a></p>
Do you or any of your co-authors have a conflict of interest to declare?	No. The authors declare no conflict of interest.
<b>Response to Reviewers:</b>	
<b>Keywords:</b>	silicon; iron-boron pairs; light-induced dissociation; wavelength impact; dissociation rate

To: physica status solidi (a) Editorial Board  
Subject: Article Submit

Dear Editors,

Enclosed with this letter you will find the electronic submission of manuscript entitled “Influence of illumination spectrum on dissociation kinetic of iron-boron pairs in silicon” by Oleg Olikh, Oleksandr Datsenko, and Serhiy Kondratenko.

It is widely recognized, that defects significantly impact semiconductor properties. Therefore it's crucial to understand the parameters of defects and the mechanisms behind their alteration, which holds significant practical importance. Over several decades, extensive knowledge has been amassed regarding specific defects, with the iron-boron pair in silicon being a well-studied example. Therefore, the discovery of new findings or the resolution of contentious issues is particularly intriguing.

It has been established that the rate of light-induced dissociation of FeB pairs is influenced by integrated illumination intensity, temperature, and the defect composition of the material. Our investigation found that the spectral composition of illumination is an additional important factor affecting dissociation efficiency. Specifically, we demonstrated that increased photon energy leads to higher photo-dissociation efficiency. The results indicate that the recombination-enhanced defect reaction is the more probable mechanism at the second stage of light-induced dissociation, as opposed to iron ion recharge. We are confident that this study, shedding new light on the long-studied FeB pair in silicon, will be of significant interest to your readers.

The corresponding abstract has been accepted for poster presentation at the 20th Conference on Gettering and Defect Engineering in Semiconductor Technology (GADEST 2024, Reference ID 105868).

This is an original paper which has not been simultaneously submitted as a whole or in part anywhere else. No elements of the work have been published in any form. No conflict of interest exists in the submission of this manuscript.

We would very much appreciate if you would consider the manuscript for publication in the GADEST 2024 special issue in *physica status solidi (a)*.

Sincerely yours,  
Oleg Olikh and co-authors.  
Taras Shevchenko National University of Kyiv  
Kyiv 01601, Ukraine  
E-mail: olegolikh@knu.ua

Dear Editor,

We like to express our appreciation to the reviewers for their comments. We are resubmitting the revised version of the paper number pssa.202400351. We have studied the comments of the reviewer carefully, and have changed the text according to the comments they have listed. The location of revisions is pointed by blue in "RevisedMarkedManuscript.pdf". Below we refer to each of the reviewer's comments.

## Response to Reviewer #1

**Comment 1.** *The authors could consider mentioning where does the iron come to the samples? Is it in the wafers to begin with after the crystal growth or is some intentional iron contamination done prior to device processing? In my opinion this information would be worth mentioning in the manuscript.*

**Reply:** The technological process of solar cells (SCs) manufacturing from Cz-p-Si wafers included the formation of separating and isotype barriers ( $n^+$ - $p$  and  $p$ - $p^+$  junctions) by diffusion of phosphorus ( $\text{POCl}_3$ ) and boron ( $\text{BCl}_3$ ) from the gas phase, respectively; thermal oxidation; thermal annealing; photolithography; etching the dividing groove; chemical treatments; magnetron sputtering of aluminum contacts to the front and back sides.

It has been found that some SC lots have significantly worse parameters compared to typical solar cells for this technological process. In particular, the photoconversion efficiency was almost halved. The analysis showed that the reason for such a deterioration in the SC parameters is a sharp drop in the diffusion length of minority charge carriers (electrons)  $L_n$  in the SC base. Additional experiments with thermal annealing at temperatures of 200°C and 90°C (the procedure is described by Tayyib *et al.*[1]) showed that the decrease in  $L_n$  value is caused by iron impurities available in the SC base at concentrations up to  $4 \cdot 10^{13} \text{ cm}^{-3}$ . It has also been found that the source of iron impurity is insufficiently pure chemicals that were used for chemical treatments in the technological process, obtained from another supplier. These reagents were the source of contamination in the process of manufacturing experimental SC samples.

At the same time, such detailed information about the samples has already been provided in a previous paper [2]. Therefore, in revised manuscript, we briefly describe the causes of contamination and provide links to a more comprehensive description — see page 9, paragraphs 5.

**Comment 2.** *What was the size of the samples and solar cells used in the experiments? Was the whole sample/cell surface illuminated during the experiments or just part of it locally?*

**Reply:** The area of the samples used in the study was  $1 \times 1 \text{ cm}^2$ . The entire surface of the solar cell was illuminated during the experiments.

This answer is incorporated in the text on page 9, paragraph 6.

**Comment 3.** *Based on the reported sheet resistance values, the emitter and back surface field diffusions are quite heavy and could thus act as strong gettering sinks for iron during the device processing. Could the authors comment on this? This could lead to rather uneven distribution of iron in the samples and also the iron being in different forms in different locations. Does this affect the results and if yes, how? (Perhaps here the fact that the light used in the IV-measurements was monochromatic with a wavelength of 940 nm plays a role.)*

**Reply:** Really, phosphorus diffusion [3] and implantation [4, 5] gettering are well-known methods to relocate iron from the bulk to the emitter, where it is less harmful. Therefore, due to creating barriers (see Reply to Comment 1), the concentration of iron near the surfaces of the solar cell could have increased. However, gettered iron is not recombination-active like  $\text{Fe}_i$  or  $\text{FeB}$ , and even high amounts of gettered iron do not increase emitter recombination [3].

Thus, only the fraction of iron remaining in the bulk could respond to illumination in our experiments. Considering that other high-temperature process operations (thermal oxidation, thermal annealing) were performed after the formation of barriers, we believe that the bulk iron is evenly distributed. Previous studies have not reported uneven distribution of iron due to phosphorus-induced gettering, and the possibility of uneven distribution was not considered in the analysis of the light-induced kinetics of iron-boron pairs [4, 5].

Additionally, for light with a wavelength of 940 nm, the absorption depth is approximately 50 μm at 340 K [6]. Therefore, using monochromatic light as a probe tool primarily allowed us to focus on processes deep within the solar cell base.

**Comment 4.** *Keeping in mind the cell structure including e.g. strong emitter and BSF diffusions, the reported value of  $\tau_{\text{au\_other}}$  (2.2 ms) seems quite high. Could the authors comment on this? Were there any uncontaminated reference cells included in the experiments? (These would perhaps be good references also elsewhere in the manuscript.) Was their lifetime characterized to back up this claim and the resulting validity of  $\tau_{\text{au\_other}}$  being much higher than  $\tau_{\text{au\_feb}}$ ?*

**Reply:** First and foremost, we would like to apologize for the inaccuracy. The cited value of 2.2 μs corresponds to the lifetime associated with Shockley-Read-Hall recombination at Fe-related defects. The information in the revised manuscript

has been rephrased for clarity — see page 4, paragraph 2.

During fitting the time dependencies of short-circuit current, the following expression was used to estimate the minority carrier lifetime in the base  $\tau$ :

$$\frac{1}{\tau(t)} = \frac{1}{\tau_i} + \frac{1}{\tau_{SRH}^{Fe_i}(t)} + \frac{1}{\tau_{SRH}^{FeB}(t)} + \frac{1}{\tau_{other}}, \quad (1)$$

where  $\tau_i$  is the lifetime associated with intrinsic recombination,  $\tau_{SRH}^{Fe_i}$  and  $\tau_{SRH}^{FeB}$  are related to the recombinations at interstitial iron atoms  $Fe_i$  and at FeB pairs, accordingly;  $\tau_{other}$  describes further recombination channels (other impurities, lattice defects, surface recombination).

It turned out that the final term in Eq. (1) is significantly smaller than the preceding ones. This fact gave grounds to assert that  $\tau_{other}$  significantly exceeds  $\tau_{FeB}$ .

For other samples of the same series with a lower iron concentration (and a lower  $\tau_{other}/\tau_{FeB}$  ratio), the  $\tau_{other}$  value was estimated more accurately. Thus, the measurements showed that for solar cells with  $N_{Fe,tot} = (1.8 \times 10^{11} - 1.4 \times 10^{12}) \text{ cm}^{-3}$ , the bulk lifetime ranged from 20 to 300  $\mu\text{s}$ , and no correlation was observed between the values of  $N_{Fe,tot}$  and  $\tau_{other}$ .

The last part of answer is incorporated in the text on page 4, paragraph 2.

**Comment 5.** *Was the iron concentration in the samples/cells verified with some of the well-established methods for iron concentration determination such as surface photovoltage method (SPV)? That would provide also simultaneously a good reference value for the diffusion length value determined in the manuscript.*

**Reply:** We must acknowledge that additional verification of the iron concentration was not carried out for the solar cell used in this work. However, the approach to determining the iron concentration from the short-circuit current kinetics was initially validated by assessing the diffusion length [7]. The results obtained by different methods were well-agreed, as described in previous papers [2, 8].

It should be noted that even some inaccuracy in iron concentration evaluation could have affected only the absolute values of the coefficient  $K$ , which are reported [9, 10, 5] with a big enough scatter. The primary study's conclusion (the dependence of the dissociation rate and  $K$  on the illumination spectrum) remains unchanged.

**Smaller Comment 1.** *The authors could consider moving the experimental from the end to the second section in the paper. There is a lot of crucial information in the experimental part that is needed to understand the results properly. Therefore, it could be very useful for the readers to read the experimental part first before going into the results section.*

**Reply:** Overall, we also support the opinion that the ability to read the experimental part first before going into the results section is useful, customary, and fully justified. However, in this case, we must adhere to the “Guide for Authors” and the L<sup>A</sup>T<sub>E</sub>X template which state that the order of the sections must be as follows: “Title – Author(s) – (Dedication) – Affiliation(s), – Keywords – Abstract – Main text – (Experimental/Methods Section) – Acknowledgements – References – (Biographies) – Table of Contents text [Sections in brackets are only present in certain article types]”.

**Smaller Comment 2.** *The paper would benefit from one round of language and typo checks. There were quite a lot of such problems all around the paper. Here are just some examples:*

*Title: Should it be dissociation kinetics and not kinetic?*

*Page 1, line 42: “and have a solid understanding of some defects”. Something wrong in this sentence, should it be e.g. “and that there is a solid understanding of some defects.”*

*Page 4, lin49: “the lifetime associated with... (about 2.2  $\mu\text{m}$ )” Unit wrong, should be ms?*

*Page 6, line 29: “These behaviour...” Should be This behaviour?*

*Figure 5 caption: “carrier generate rate”*

*etc.*

**Reply:** We apologize for any language errors. A bilingual speaker has revised the text, and we hope it shows improvement.

The reviewer is completely correct and

- title revised to “Influence of Illumination Spectrum on Dissociation Kinetics of Iron-boron Pairs in Silicon
- sentence revised to “Nevertheless, it must be noted that considerable data have been amassed on silicon, resulting in a solid understanding of certain defects.” (page 1, paragraphs 2)
- correct unit is  $\mu\text{s}$  (page 4, paragraphs 2)
- the correct beginning of sentence is “This behavior...” (page 6, paragraphs 2)

- “carrier generate rate” in Figure 5 caption is replaced by “carrier generation rate” (page 7).

Other numerous corrections are highlighted in blue in “RevisedManuscript.pdf”.

## Response to Reviewer #2

**Comment 1.** Grammatical error in the last sentence of the abstract.

**Reply:** The revised last sentence in the abstract reads:

“The results indicate that recombination-enhanced defect reaction is the primary factor in the second stage of pair dissociation.”

The manuscript has been revised. We sincerely hope to see a significant decrease in grammatical errors.

**Comment 2.** Figure1 and TOC, it looks nice, but it is difficult to understand. Authors need to add inputs and outputs. One of outputs will be K values. For example, add an arrow coming out from the box named “Discussion & Conclusion”, and write K. Otherwise, readers will not understand what is this figure for. Page2, Line40, there is an explanation of “First step”. I do not find “Second step”.

**Reply:** The Figure 1 has been modified according to the Reviewer’s suggestions. Additionally, the boxes in the figure have been numbered, and these numbers are referenced in the updated description (page 2, paragraph 4).

**Comment 3.** A main result is that K values depends on the light source, namely spectral shape. These values were obtained by fitting equation(1) to the plot in Fig. 6(a). I have a doubt that K should not change by experimental condition. It is an intrinsic constant. For the fitting, N\_FeB was assumed to be constant in the manuscript, but it may not.

**Comment3 is critical. Explanations are required.**

**Reply:** For us, it was also somewhat surprising that  $K$ , which was considered a material constant, depended on illumination parameters. However, from a physical point of view, such dependence is not entirely incomprehensible. Indeed, according to the recombination-enhanced defect reaction, electron–phonon interactions during the dissociation of FeB pairs lead to the athermal diffusion of iron ions [5, 11]. The increase in the number of phonons due to the thermalization of photoelectrons, which occurs when higher energy photons are absorbed, should intensify the electron-phonon interaction process. Such a phenomenon is observed in the experiment and causes changes in the value of  $K$ , which integrally characterizes the dissociation process of the pairs.

Regarding the fitting where the concentration of pairs was assumed to be constant, the study presents results obtained under the illumination of a single solar cell at a constant temperature (340 K). Before strong illumination, the sample was kept in the dark for an extended period.

Therefore, there is no reason to expect that the total concentration of defects or the ratio between the amounts of FeB and Fe<sub>i</sub> would change. Moreover, this was verified in the experiment (see Table 1, last column).

**Comment 4.** A unit “cm<sup>3</sup>” is in equation(5). It should not be.

**Reply:** We respectfully disagree with the Reviewer. On one hand, the factor of  $5.7 \times 10^5$  corresponds precisely to the case when the unit of acceptor–doping concentration is cm<sup>-3</sup> [10, 5, 12]. On the other hand, since the temperature unit is Kelvin and the unit of  $p$  is cm<sup>-3</sup>, the factor  $\left(\frac{1}{K \text{ cm}^3} \cdot \frac{T}{p}\right)$  is dimensionless. Thus, the expression

$$R_a^{-1} = 5.7 \times 10^5 \frac{s}{K \text{ cm}^3} \times \frac{T}{p} \exp\left(\frac{E_m}{kT}\right) \quad (2)$$

has the dimension of time.

**Comment 5.** I did not find where Eq.(3) and (4) are used. Exactly the same equations are in the cited articles. These equations and related sentences can be deleted so that readers can easily understand the content.

**Reply:** We fully understand that it is not good practice to disagree with the reviewer; however, we kindly request permission to retain the equations. Eq. (3) is needed to demonstrate a relationship between the fitting parameters of the experimental curve (Figure 3) and defect characteristics — see page 4, paragraph 6. Eq. (4) allows for an easy and understandable entering of  $t_{dark}$  (time after stopping strong illumination), which is extensively used throughout the text and figures.

Additionally, the equation directly relates to the time dependence of the recovery of the short-circuit current (Fig. 2a) and is mentioned on page 2, second paragraph from the bottom.

While references to cited articles can be sufficient, we believe that including Eq.(3) and (4) enables readers to clearly understand the connection between the experiment and the FeB characteristics within the study framework.

Sincerely yours,  
Oleg Olikh, Oleksandr Datsenko, and Serhiy Kondratenko.  
Taras Shevchenko National University of Kyiv  
Kyiv 01601, Ukraine  
E-mail: olegolikh@knu.ua

## References

- [1] M. Tayyib, J. Theobald, K. Peter, J. Odden, T. Sætre, *Energy Procedia* **2012**, 27 21 , proceedings of the 2nd International Conference on Crystalline Silicon Photovoltaics SiliconPV 2012.
- [2] O. Olikh, V. Kostylyov, V. Vlasiuk, R. Korkishko, Y. Olikh, R. Chupryna, *J. Appl. Phys.* **2021**, 130, 23 235703.
- [3] V. Vähänissi, A. Haarahiltunen, H. Talvitie, M. Yli-Koski, H. Savin, *Prog. Photovoltaics Res. Appl.* **2013**, 21, 5 1127.
- [4] H. S. Laine, V. Vähänissi, A. E. Morishige, J. Hofstetter, A. Haarahiltunen, B. Lai, H. Savin, D. P. Fenning, *IEEE Journal of Photovoltaics* **2016**, 6, 5 1094.
- [5] N. Khelifati, H. S. Laine, V. Vähänissi, H. Savin, F. Z. Bouamama, D. Bouhafs, *Phys Status Solidi A* **2019**, 216, 17 1900253.
- [6] M. A. Green, *Prog. Photovoltaics Res. Appl.* **2022**, 30, 2 164.
- [7] G. Zoth, W. Bergholz, *J. Appl. Phys.* **1990**, 67, 11 6764.
- [8] O. Olikh, V. Kostylyov, V. Vlasiuk, R. Korkishko, R. Chupryna, *J. Mater. Sci.: Mater. Electron.* **2022**, 33, 16 13133.
- [9] L. J. Geerligs, D. Macdonald, *Appl. Phys. Lett.* **2004**, 85, 22 5227.
- [10] C. Möller, T. Bartel, F. Gibaja, K. Lauer, *J. Appl. Phys.* **2014**, 116, 2 024503.
- [11] L. Kimerling, J. Benton, *Physica B+C* **1983**, 116, 1 297.
- [12] J. Tan, D. Macdonald, F. Rougieux, A. Cuevas, *Semicond Sci. Technol.* **2011**, 26, 5 055019.

# <sup>1</sup> Influence of Illumination Spectrum on Dissociation Kinetics<sub>S</sub> of <sup>2</sup> <sup>3</sup> Iron-boron Pairs in Silicon

<sup>5</sup> Oleg Olikh\* Oleksandr Datsenko Serhiy Kondratenko

<sup>9</sup> Prof. O. Olikh, Dr. O. Datsenko, Prof. S. Kondratenko

<sup>10</sup> Taras Shevchenko National University of Kyiv, 64/13, Volodymyrska Street, 01601, Kyiv, Ukraine

<sup>11</sup> Email Address: olegolikh@knu.ua

<sup>13</sup> Keywords: *silicon, iron-boron pairs, light-induced dissociation, wavelength impact, dissociation rate*

<sup>15</sup> Photo-dissociation kinetics of iron–boron (FeB) pairs in boron-doped Czochralski silicon was studied experimentally using different  
<sup>16</sup> light sources. It was shown that the FeB dissociation rate depends not only on integrated light intensity and overall carrier genera-  
<sup>17</sup> tion rate, but also on spectral composition of illumination. The value of the material constant of dissociation  $K$  varies and has been  
<sup>18</sup> determined to be within  $(1.5 - 3.8) \times 10^{-15}$  s. The investigation has revealed an increase in the dissociation rate with increase in  
<sup>19</sup> photon energy. The results indicate that recombination-enhanced defect reaction is the primary factor in the second stage of pair  
<sup>20</sup> dissociation.

<sup>21</sup>

<sup>22</sup>

## <sup>23</sup> 1 Introduction

<sup>25</sup> Defects significantly impact semiconductor properties. Although when minimizing device dimensions to  
<sup>26</sup> nanometers, focus some shifts from extended to point defects, physical properties still rely heavily on  
<sup>27</sup> the presence and distribution of these irregularities. Hence, many strategies for enhancing semiconduc-  
<sup>28</sup> tor structures, including radiation and temperature treatments or certain fabrication conditions, strive  
<sup>29</sup> to decrease the defect concentration or neutralize its effects [1, 2, 3]. For instance, in the case of photo-  
<sup>30</sup> voltaic devices, we must understand and optimize the carrier properties related to defects and impurities  
<sup>31</sup> [1]. Such controlled alteration methods of the defect subsystem have been generalized under the term  
<sup>32</sup> “defect engineering” and are extremely important from a practical standpoint.

<sup>35</sup> Successful defect engineering hinges on an in-depth understanding of defect properties. Key factors are  
<sup>36</sup> defect formation energy, transition energy levels, self-compensating effects, nonradiative recombination  
<sup>37</sup> caused by defects, and the mechanism of reconstruction and diffusion [1]. Considering the extraordinary  
<sup>38</sup> diversity of possible intrinsic and impurity defects, information on them is incomplete, even for silicon,  
<sup>39</sup> which is the most studied semiconductor. Nevertheless, it must be noted that considerable data have  
<sup>40</sup> been amassed on silicon, resulting in a solid understanding of certain defects [4].

<sup>43</sup> For instance, iron impurity and iron-boron pairs are such defects that they are common, detrimental,  
<sup>44</sup> and often unavoidable contaminants in photovoltaic silicon [3, 5]. Specifically, iron atoms are known to  
<sup>45</sup> be at the interstitial sites, and  $\text{Fe}_i^+$  are highly efficient recombination centers [6]. In p-type Si at room  
<sup>46</sup> temperature, iron atoms are almost predominantly bound into complexes with dopants (B, Ga, Al, In).  
<sup>47</sup> This defect demonstrates bistable behavior: the stable state is defined by the configuration in which Fe  
<sup>48</sup> occupies the first nearest tetrahedral interstitial site closest to the substituent atom, whereas, in the metastable  
<sup>49</sup> configuration, Fe is at the second  $T_d$  interstitial site [7]. The energy levels associated with iron and its  
<sup>50</sup> complexes, as well as the respective carrier capture cross-sections, are well established [4, 8]. Among the  
<sup>51</sup> acceptor-iron pairs, the complex FeB is the most thoroughly investigated, primarily due to the widespread  
<sup>52</sup> use of Si:B in fabricating various devices, such as solar cells. However, it is worth mentioning that gal-  
<sup>53</sup> lium is gaining more and more attention as an acceptor dopant whose incorporation, for instance, can  
<sup>54</sup> help mitigate light and elevated temperature-induced degradation [9].

<sup>57</sup> The dynamics of FeB pairs are also examined. It's established that FeB pairs can be dissociated through  
<sup>58</sup> illumination, minority carrier injection, and thermal treatment at 200 °C [10]. In the context of illumina-  
<sup>59</sup> tion, the dissociation rate  $R_d$  is influenced by the overall carrier generation rate  $G$  [11, 10, 12, 13]:

$$\text{62} \quad R_d = K \left( \frac{G}{N_{\text{FeB}}} \right)^2, \quad (1)$$

<sup>63</sup>

<sup>64</sup>

<sup>65</sup>

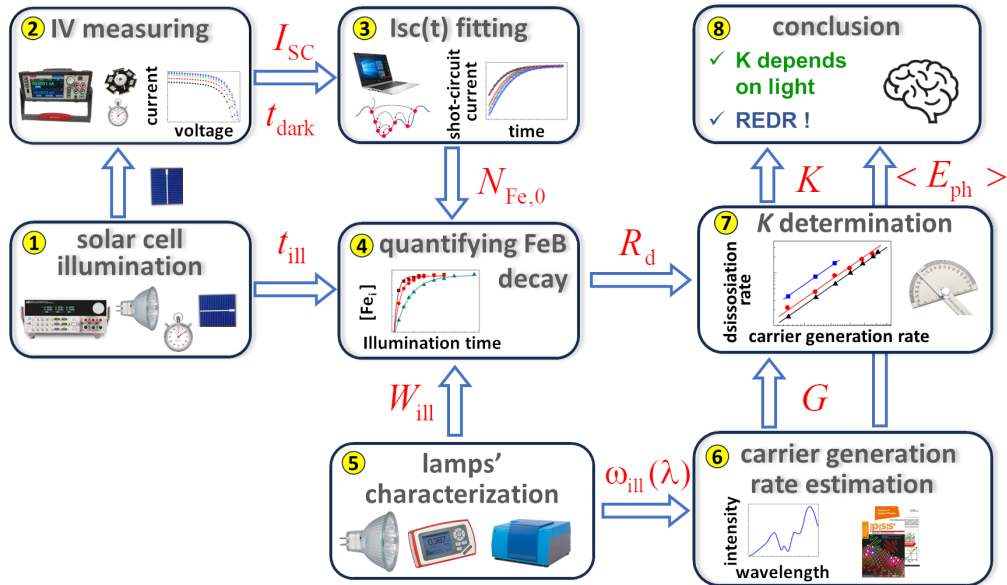


Figure 1: Investigation framework

where  $N_{FeB}$  is the pair concentration,  $K$  is the constant of the material. It is necessary for the illumination power to exceed  $0.1 \text{ W cm}^{-2}$  to achieve almost complete dissociation of the FeB pairs [14]. The dissociation process of FeB pairs by electron capture unfolds in two stages [15, 10]: the initial one involves the neutralization of Fe and the elimination of the Coulomb attraction between the pair components. The mechanism of the second stage is contentious; it may involve either the recharge of the iron ion or the recombination-enhanced defect reaction (REDR) triggered by electron-hole recombination. It should be noted that despite the extensive data on the properties of iron-related defects in silicon, intensive research continues. In particular, efforts focus on analyzing the impact of high-intensive illumination [16] or dopant compensation [17], alongside clarifying the second-stage mechanism of dissociation [5] or reassessing recombination parameters [18].

This study aims to investigate the effect of the light spectrum on the dissociation kinetics of FeB pairs in silicon. While pair dissociation is typically carried out using a halogen lamp [11, 5] or a 904 nm laser [16, 10, 19], there is limited understanding of how the light source influences this process. By studying the impact of different illumination spectra on FeB dissociation, we aim to provide valuable insights for defect engineering and the efficient transformation of detrimental impurity iron atoms into a highly mobile interstitial state within the active region of a silicon device. Besides, such information, in our opinion, can help make the right choice between existing options for the second stage of pair decay.

In Figure 1, the main stages of the research are illustrated. First step was the determination of the dissociation rate of FeB pairs under illumination with different integral intensities. Three light sources from different manufacturers were used (box 1 on Figure 1, further details are described in Section 4). The kinetics of short-circuit current were used (boxes 2 and 3) to measure the number of interstitial iron atoms formed over fixed time under intense illumination (box 4). The result is presented in Subsection 2.1. Second step and Subsection 2.2 deal with estimating the carrier generation rate using spectra of sample illumination (box 5) and considering the effects of light reflection, absorption by free carriers, and effective absorption depths (box 6). The results showed that light-induced dissociation efficiency increases with decreasing photon wavelength — see Subsection 2.3 and box 7. Finally, we conclude this paper in Section 3 (box 8).

## 1 2 Results and Discussion

### 2 2.1 Dissociation rate determination

5 The equilibrium between free  $\text{Fe}_i$  and  $\text{Fe}_i\text{B}_{\text{Si}}$  is known to be determined by the following equations [20,  
6 5, 10]



10 where  $R_a$  is the association rate. As a result, the concentration of unpaired interstitial iron atoms  $N_{\text{Fe}_i}$   
11 depending on illumination time  $t_{\text{ill}}$  during light-induced dissociation can be described as follows [11, 12,  
12 21]

$$14 \quad N_{\text{Fe}_i}(t_{\text{ill}}) = \left( N_{\text{Fe,eq}} - N_{\text{Fe,tot}} \frac{R_d}{R_d + R_a} \right) \exp[-(R_d + R_a)t_{\text{ill}}] + N_{\text{Fe,tot}} \frac{R_d}{R_d + R_a}, \quad (3)$$

17 where  $N_{\text{Fe,tot}}$  is the total concentration of the impurity iron,  $N_{\text{Fe,eq}}$  represents the concentration of un-  
18 paired interstitial iron atoms in the equilibrium state (in darkness,  $N_{\text{Fe,eq}} = N_{\text{Fe}_i}(t_{\text{ill}} \leq 0)$ ). It is impor-  
19 tant to highlight that  $N_{\text{Fe,eq}}$  is significantly influenced by temperature and the Fermi level location [20].  
20 Specifically, in the case of p-type Si with a hole concentration  $p = 1.36 \times 10^{15} \text{ cm}^{-3}$  (which corresponds  
21 to the structure under investigation), at a temperature of  $T = 300 \text{ K}$ ,  $N_{\text{Fe,eq}}$  is about 1 percent of  $N_{\text{Fe,tot}}$ ,  
22 which is negligible for practical considerations. However, when the temperature rises to 340 K, the pro-  
23 portion of  $N_{\text{Fe,eq}}$  increases to approximately 14.5%.

25 After stopping the illumination, only the process of association occurs, and the time dependence of  $\text{Fe}_i$   
26 concentration can be expressed as follows [20, 22]:

$$28 \quad N_{\text{Fe}_i}(t_{\text{dark}}) = (N_{\text{Fe,0}} - N_{\text{Fe,eq}}) \times \exp(-R_a t_{\text{dark}}) + N_{\text{Fe,eq}}, \quad (4)$$

30 where  $t_{\text{dark}}$  is the time after stopping the intense illumination,  $N_{\text{Fe,0}}$  is the concentration of interstitial  
31 iron atoms formed after illumination,  $N_{\text{Fe,0}} = N_{\text{Fe}_i}(t_{\text{dark}} = 0) = N_{\text{Fe}_i}(t_{\text{ill}})$ .

32 The study examined the dependence of  $N_{\text{Fe,0}}$  in silicon solar cells on illumination time  $t_{\text{ill}}$  using different  
33 integral illumination intensities  $W_{\text{ill}}$  (200 – 750 mW) and light sources (three halogen lamps labeled as  
34 Orion, Osram, and GE and described in detail in Section 4). The experiments were conducted at a tem-  
35 perature of 340 K. The values of  $N_{\text{Fe,0}}$  were determined using a methodology [23, 21] based on fitting the  
36 kinetics of short-circuit current  $I_{SC}$  under low-intensity monochromatic illumination. Specifically, after  
37 intense illumination with a duration of  $t_{\text{ill}}$ , the current-voltage characteristic ( $I$ - $V$ ) of the solar cell was  
38 measured every 21 seconds over a time  $t_{\text{dark}}$  of about 3000 seconds.

39 **Figure 2a** shows some typical  $I$ - $V$  curves. A gradual increase in both the short-circuit current and the  
40 open-circuit voltage is observed after the cessation of illumination. This indicates a decrease of the re-  
41 combination activity of the defect subsystem, which is a result of the transition of interstitial iron to the  
42 bound state with the acceptor. Moreover, negligible changes in the  $I$ - $V$  curves at the end of the mea-  
43 surement interval denote that the selected interval of 50 minutes is sufficient for complete association.

44 **Figure 2b** illustrates the dependencies  $I_{SC}(t_{\text{dark}})$  after the illumination with different intensities. As  
45 shown previously [21], the magnitude of the change in  $I_{SC}$  after the dark recovery period inherently cor-  
46 relates with the concentration of  $\text{Fe}_i$  formed due to the light-induced dissociation of  $\text{FeB}$  pairs. The pre-  
47 sented data evidence that the rise of  $W_{\text{ill}}$  leads to an increment in the dissociation efficiency. Meanwhile,  
48 the recovery time remains insensitive to the illumination parameters, which is expected, as the former is  
49 determined by  $R_a$  (see Equation (4)).

50 It should be noted that apart from  $N_{\text{Fe,0}}$ , the fitting of short-circuit current [23, 21] allows for the esti-  
51 mation of the migration energy of  $\text{Fe}_i$ ,  $E_m$ , and bulk lifetime  $\tau_{\text{other}}$  of minority carriers, which is related  
52 to recombination channels other than Fe-related defects and intrinsic recombination. The obtained value  
53  $E_m = (0.650 \pm 0.005) \text{ eV}$  coincides with that known from Refs. [12, 24, 25]. This coincidence confirms  
54 that the investigated processes are indeed associated with rebuilding, as Equation (2) describes. In turn,  
55 the value of  $E_m$  allows for the estimation of the association rate [10, 12, 24]:

$$62 \quad R_a^{-1} = 5.7 \times 10^5 \frac{\text{s}}{\text{K cm}^3} \times \frac{T}{p} \exp\left(\frac{E_m}{kT}\right). \quad (5)$$

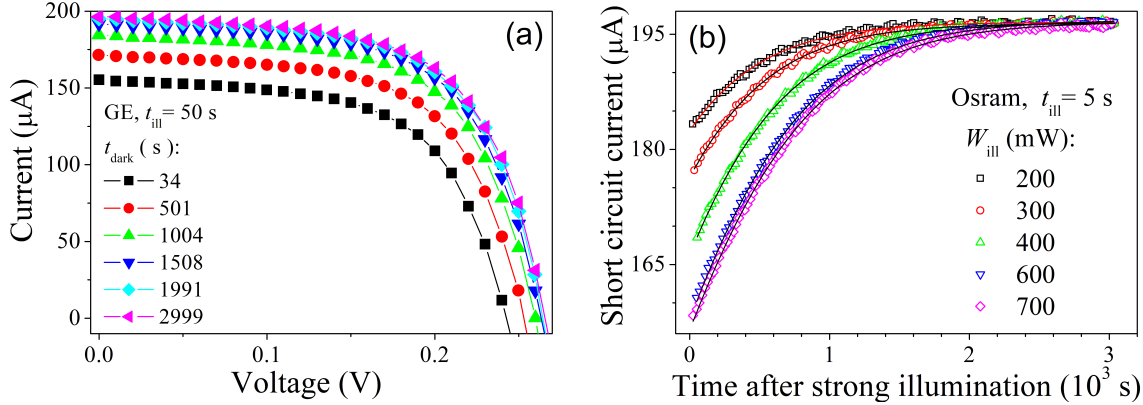


Figure 2: Typical  $I$ - $V$  characteristics measured at  $T = 340$  K under low-intense LED illumination at 940 nm after delays following the exposure for 50 s to intense (400 mW) light (GE lamp) (a) and short circuit current vs the delay time after the illumination for 5 s of Osram lamp with various intensities (b). The marks are the experimental data, and the lines on (b) are the fitting curves according to [23, 21].

Thus, in our case,  $R_a = (1.68 \pm 0.03) \times 10^{-3}$  s<sup>-1</sup>.

As for the value of  $\tau_{\text{other}}$ , it was found to exceed significantly the lifetime associated with Shockley–Read–Hall (SRH) recombination on Fe-related defects. The last one is about 2.2 μs, whereas  $\tau_{\text{other}}$  equals (20 – 300) μs for the samples of the same series. Notably, according Möller *et al.* [10], such a condition is essential for accurately determining the constant  $K$ , which is included in Equation (1).

The dependencies of the concentration of interstitial atoms on illumination time are shown in Figure 3. It is evident from the data that the pair dissociation rate is influenced significantly by the illumination intensity for all the used light sources. Nonetheless, the pair dissociation rate is not determined by the  $W_{\text{ill}}$  value only. As demonstrated in Figure 3d, pair dissociation under the GE source is the fastest. With Osram under otherwise identical conditions, the process is slower, while illumination with Orion proves to be the least effective in terms of altering the state of FeB pairs.

Considering Equation (3), the experimentally obtained dependencies  $N_{\text{Fe},0}(t_{\text{ill}})$  were fitted using the function

$$N_{\text{Fe},0}(t_{\text{ill}}) = A \exp(-t_{\text{ill}}/\tau_{\text{dis}}) + B, \quad (6)$$

where  $\tau_{\text{dis}}$  is the characteristic dissociation time, and  $B$  means the concentration of dissociated pairs at the saturation. The fitting parameters are collected in Table 1, including the coefficient of determination  $R^2$ . The high values of  $R^2$  (greater than 0.99) confirm the suitability of the chosen fitting formula. One can see from Equations (3) and (6) that the fitting parameters relate to defect characteristics:

$$\tau_{\text{dis}}^{-1} = R_a + R_d, \quad (7)$$

$$B = N_{\text{Fe,tot}} \frac{R_d}{R_d + R_a}. \quad (8)$$

The fitting parameters with considering the association rate of  $1.68 \times 10^{-3}$  s allow us to calculate the values of  $N_{\text{Fe,tot}}$  and  $R_d$ , which are also collected in Table 1. As seen, the calculated values of the impurity iron atom concentration  $N_{\text{Fe,tot}} = (8.7 \pm 0.1) \times 10^{12}$  cm<sup>-3</sup> are expectably independent of the light source and illumination intensity  $W_{\text{ill}}$ . This confirms the accuracy of the analysis. Contrariwise, the FeB dissociation rate may vary significantly with both the intensity value and the used light source.

According to Wijaranakula [20], the concentrations of interstitial iron atoms  $N_{\text{Fe,eq}}$  and FeB pairs  $N_{\text{FeB}}$  before the illumination at the specified value of  $N_{\text{Fe,tot}}$  and  $T = 340$  K are  $1.3 \times 10^{12}$  cm<sup>-3</sup> and  $7.4 \times 10^{12}$  cm<sup>-3</sup>, respectively. The values of  $N_{\text{Fe,eq}}$  and  $N_{\text{FeB}}$  were used to estimate the minority carrier diffusion length  $L_n$  in the base of the used solar cell. It was assumed that the dominant recombination processes are SRH recombination at  $\text{Fe}_i$  and FeB and intrinsic recombination. The required value of electron mobility  $\mu_n$  was taken from Klaassen [26], the capture cross sections and energy levels for  $\text{Fe}_i$  and FeB from Rougier *et al.* [8], the parameters of band-to-band radiative recombination and Auger recombination from Niewelt *et al.* [27] and Black & Macdonald [28], respectively. The calculated value was

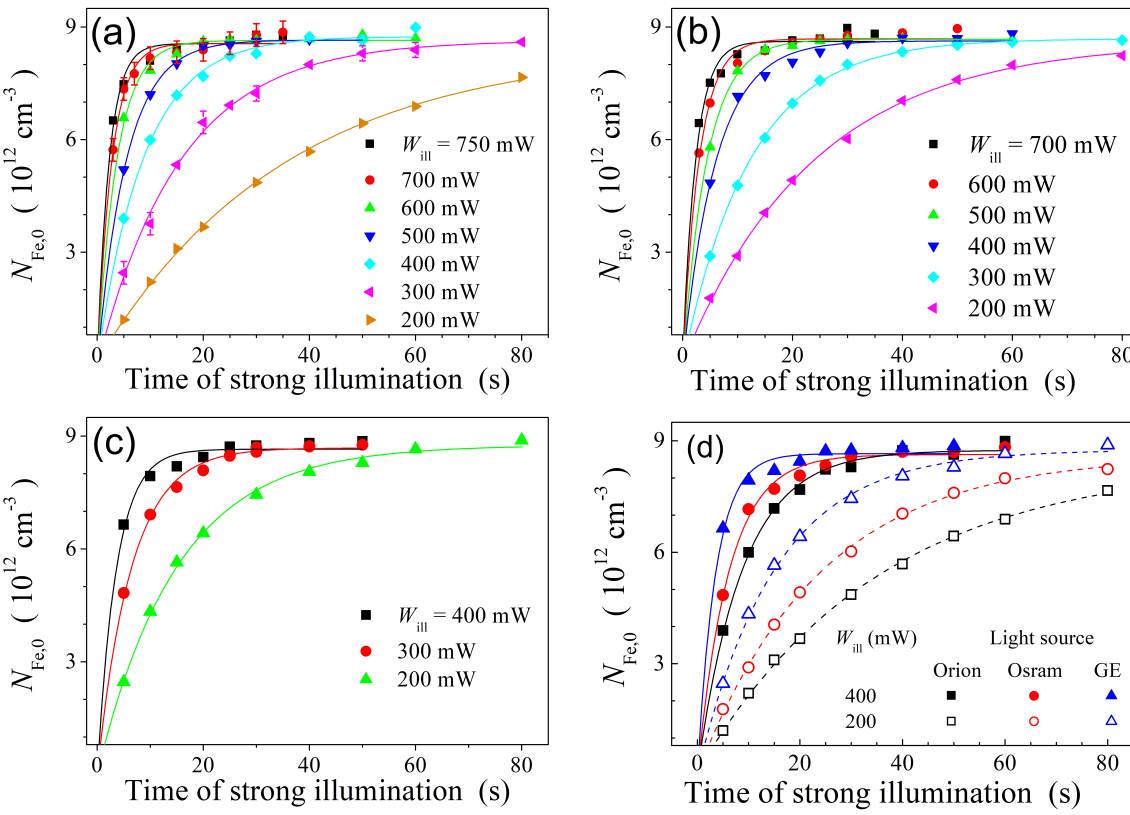


Figure 3: Rise of the dissociated FeB pair concentration under the illumination by sources Orion (a), Osram (b), GE (c) of different intensities ( $T = 340$  K). Panel (d) compares the effect of different light sources. The marks are the experimental results, the lines are the fitting by Equation (6).

34

35

36

37

38

39

40

Table 1: Fitting parameters of experimental dependencies  $N_{Fe,0}(t_{ill})$  using Equation (6) and defect parameters estimated using Equations (7-8).

$W_{ill}$ [mW]	Light source	fitting parameters			defect parameters	
		$\tau_{dis}$ [s]	$B$ [ $10^{12}$ cm $^3$ ]	$R^2$	$R_d$ [ $10^{-3}$ s $^{-1}$ ]	$N_{Fe,tot}$ [ $10^{12}$ cm $^{-3}$ ]
750	Orion	$2.2 \pm 0.2$	$8.6 \pm 0.1$	0.993	450	8.6
	Osram	$2.7 \pm 0.2$	$8.7 \pm 0.1$	0.995	370	8.7
700	Orion	$2.4 \pm 0.2$	$8.6 \pm 0.1$	0.992	410	8.6
	Osram	$3.7 \pm 0.2$	$8.65 \pm 0.06$	0.998	270	8.7
600	Orion	$3.0 \pm 0.2$	$8.69 \pm 0.08$	0.995	330	8.7
	Osram	$5.5 \pm 0.2$	$8.65 \pm 0.04$	0.999	180	8.7
500	Orion	$4.5 \pm 0.1$	$8.7 \pm 0.1$	0.998	220	8.8
	Osram	$8.8 \pm 0.3$	$8.74 \pm 0.06$	0.998	110	8.8
400	Orion	$6.1 \pm 0.2$	$8.63 \pm 0.08$	0.997	160	8.7
	Osram	$3.6 \pm 0.3$	$8.7 \pm 0.1$	0.996	280	8.7
300	Orion	$15.7 \pm 0.6$	$8.6 \pm 0.1$	0.998	62	8.8
	Osram	$12.4 \pm 0.1$	$8.69 \pm 0.02$	0.999	79	8.8
200	GE	$6.5 \pm 0.2$	$8.69 \pm 0.05$	0.998	150	8.8
	Orion	$35 \pm 3$	$8.5 \pm 0.3$	0.998	27	8.8
	Osram	$24 \pm 1$	$8.6 \pm 0.1$	0.999	40	8.9
	GE	$15.1 \pm 0.5$	$8.7 \pm 0.1$	0.999	65	8.8

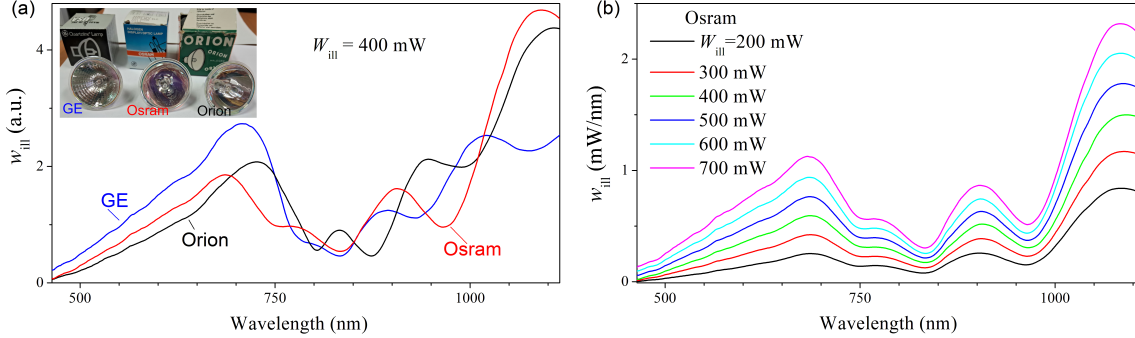


Figure 4: The spectra of sample illumination under different light sources with the same integral intensity  $W_{\text{ill}} = 400 \text{ mW}$  (a) and Osram source at various  $W_{\text{ill}}$  values (b). The inset shows photos of light sources.

found to be  $L_n = 80 \mu\text{m}$ , which is very close to  $86 \mu\text{m}$  obtained from the study of temperature dependencies of short-circuit current, see Supplementary materials.

## 2.2 Carrier generation rate estimation

The light-induced dissociation rate of FeB pairs is well known to be dependent on the carrier generation rate (see Eq. (1)). Our next aim was determining the values of  $G$  for various light sources. **Figure 4** shows the measured spectral intensity of illumination,  $w_{\text{ill}}$ , incident onto the sample surface. It is crucial to highlight that our focus is specifically on the light reaching the sample; hence, the brought spectra are distorted not only by the absorption of the lamp reflector and protective glass, but also by absorption in the fiber utilized to transmit the light flux to the solar cell. Other researchers have considered similar modifications of the illumination spectra [29]. Figure 4a displays discrepancies in the illumination spectra obtained from different light sources, attributed to variations in the operational temperatures of the halogen lamps and differences in reflectors (photos of the lamps are in the inset of Figure 4a). It is important to note that the upper limit of the spectra in Fig 4 (1120 nm) is limited by the silicon bandgap, which, according to Passler [30], corresponds to 1.11 eV at 340 K. Furthermore, Figure 4b demonstrates the change in the Osram spectrum with integral intensity increasing. Notably, in addition to the expected increase in the curve's area, a minor spectrum shift towards shorter wavelengths is observed. This behavior is typical for all used light sources.

The carrier generation rate was estimated as follows:

$$G = \int g(\lambda) d\lambda, \quad (9)$$

where the spectral density of carrier generation rate

$$g = \frac{w_{\text{ill}} \lambda}{hc} \frac{(1 - R) A_{\text{bb}}}{S d_{\text{eff}}}, \quad (10)$$

where  $n_{\text{ph}} = \frac{w_{\text{ill}} \lambda}{hc}$  is the spectral photon flux,  $R$  is the reflectance,  $A_{\text{bb}}$  is the band-to-band fraction of the absorptance,  $S$  is the illuminated area of the sample,  $d_{\text{eff}}$  is the effective width of carrier generation. When calculating the value of  $R$ , we employed an approach [31], which considers the presence of antireflective and passivating layers on the front surface of the sample, as well as the effects of multiple reflections. The resulting spectral dependence of  $R$  is shown in Figure S3 of the Supplementary materials. The expression for the e-h pair generating fraction of the Lambertian absorptance in a solar cell can be written as [32]:

$$A_{\text{bb}}(\lambda) = \frac{\alpha_{\text{bb}}}{\alpha_{\text{bb}} + \alpha_{\text{fca}}} \frac{(1 - T_r)(1 + T_r)n_r^2}{n_r^2 - (n_r^2 - 1)T_r^2}, \quad (11)$$

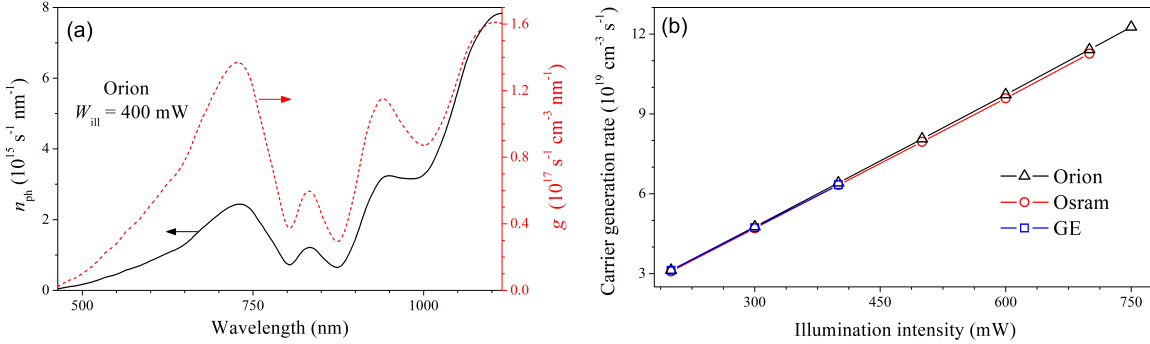


Figure 5: (a) Spectral densities of photon flux from Orion source at  $W_{\text{ill}} = 400 \text{ mW}$  (left axis, solid line) and carrier generation rate (right axis, dashed line). (b) Dependencies of carrier generation rate on illumination intensity for different light sources.

with

$$\begin{aligned} T_r &= (1 - x) \exp(-x) + x^2 E_1(x), \\ x &= (\alpha_{\text{bb}} + \alpha_{\text{fca}})d, \\ E_1(x) &= \int_x^\infty t^{-1} \exp(-t) dt, \end{aligned}$$

where  $\alpha_{\text{bb}}$  is the band-to-band absorption coefficient;  $\alpha_{\text{fca}}$  is the free carrier absorption coefficient;  $n_r$  is the refractive index;  $d$  is the width of the device.

In our calculations of  $A_{\text{bb}}$  by using Equation (11), we took  $\alpha_{\text{bb}}$  and  $n_r$  from Green[33],  $\alpha_{\text{fca}}$  from Baker-Finch *et al.* [34]. The spectral dependence of  $A_{\text{bb}}$  can be found in Supplementary materials (Figure S5). When determining the carrier generation volume, we applied the Bowden&Sinton approach [35] to thick silicon wafers, where the diffusion length or light absorption depth is significantly less than the sample thickness. In this case, the non-equilibrium carriers are concentrated near the illuminated surface, making using the arithmetic average of carrier concentration unsuitable. Therefore, the average values are calculated using carrier concentration as a weighting function, and effective generation width is determined as follows [35]:

$$d_{\text{eff}}(\lambda) = \frac{\left( \int_0^d \Delta n dx \right)^2}{\int_0^d \Delta n^2 dx}, \quad (12)$$

where  $\Delta n$  is the increase in minority carrier density due to illumination

$$\Delta n(x) = \frac{\alpha_{\text{bb}} n_{\text{ph}} L_n^2 q}{(\alpha_{\text{bb}}^2 L_n^2 - 1) k T \mu_n} \left[ \exp\left(-\frac{x}{L_n}\right) - \exp(-\alpha_{\text{bb}} x) \right]. \quad (13)$$

In calculations, we used  $L_n$  value, determined in Subsection 2.1. Figure S4 (Supplementary materials) shows some dependencies of  $d_{\text{eff}}(\lambda)$  for different  $L_n$  values.

The consideration of dependencies  $R(\lambda)$ ,  $A_{\text{bb}}(\lambda)$ , and  $d_{\text{eff}}(\lambda)$  modifies the spectral density of carrier generation rate compared to the spectrum of incident light, leading to an increased contribution to e-h pairs generated with shorter wavelengths, as illustrated in Figure 5a. In Figure 5b, variations of the total carrier generation rate  $G$  with increasing light intensity for different light sources are plotted. It is evident that differences exist between the light sources at the same  $W_{\text{ill}}$ , however, they are within 2 percent of the values; Orion source reveals the highest carrier generation rates.

Thus, the discrepancies noticed previously in the value of  $R_d$  (see Table 1) under identical illumination intensity levels cannot be attributed to variations in the carrier generation rate among different light sources, even when considering the quadratic dependency (1) of the dissociation rate on  $G$ . Hence, there must be another underlying cause for these differences.

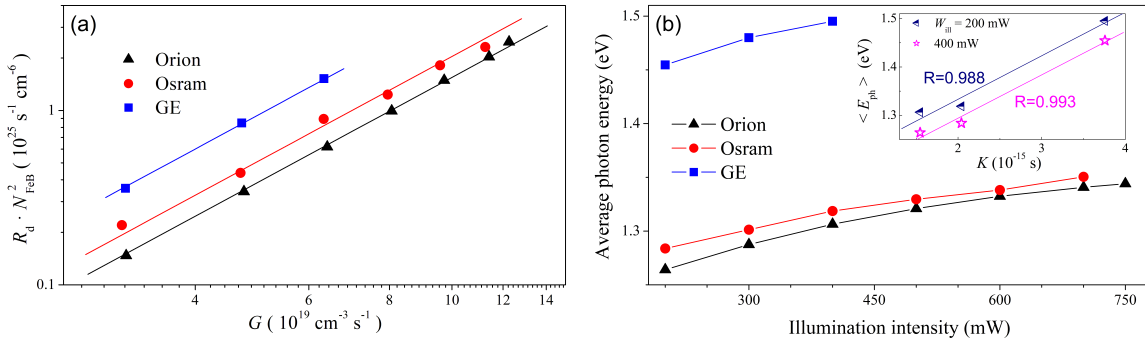


Figure 6: (a) FeB pair dissociation rate plotted as  $(R_d \cdot N_{FeB}^2)$  versus the light-induced generation rate. The solid lines are the fitting with functions  $\propto G^2$ . (b) Dependencies of average photon energy on illumination intensity for different light sources. The inset shows pre-factor  $K$  vs average photon energy for the different light sources and illumination intensities. The lines are linear fitting curves. Coefficients of correlation are shown as well.

### 2.3 Effect of illumination spectrum on FeB pair decay

The dependencies  $R_d(G)$  in the logarithmic scale are presented in **Figure 6a**. The lines are quadratic dependencies  $\propto G^2$  fitting the experimental data using Equation (1). High correlation coefficients exceeding 0.998 validate the applicability of the quadratic dependence. It should be noted that Khelifati *et al.* [12] stipulated the change of  $R_d$  to  $R_d(1 + \tau_{FeB}/\tau_{other})^2$  ( $\tau_{FeB}$  is the lifetime associated with recombination on FeB pairs) on the left side of Equation (1). However, in our case  $\tau_{other} \gg \tau_{FeB}$ , as mentioned in Subsection 2.1, therefore, this additional multiplier may be neglected.

The prefactor  $K$  values determined from the fitting are  $3.8 \times 10^{-15} \text{ s}$  for the GE light source,  $2.0 \times 10^{-15} \text{ s}$  for the Osram, and  $1.5 \times 10^{-15} \text{ s}$  for the Orion source.  $K$  is an important parameter related to the phenomenon of FeB pair dissociation caused by illumination [12], and the values obtained in this study are comparable to those ( $4.2 \times 10^{-17} - 5 \times 10^{-15} \text{ s}$ ) presented in other studies [11, 10, 12]. It is worth noting that the variety of the constant  $K$  values for diverse samples in prior research was attributed to variations in defect composition and the presence of alternative recombination channels apart from iron-related defects [11, 10]. It should be noted that  $R_d$  is known to be temperature-dependent [36]. However, our values of  $K$  were obtained for the same structure under identical conditions, including temperature and integrated light intensity.

So, the obtained data indicate that, when analyzing light-induced dissociation of FeB pairs, it is necessary to consider not only the quantity of photo-generated charge carriers, but also the energies of the photons that lead to their appearance. For such an energy characterization of light sources, we used the average photon energy  $\langle E_{ph} \rangle$ :

$$\langle E_{ph} \rangle = \frac{\int \frac{hc}{\lambda} n_{ph}(\lambda) d\lambda}{\int n_{ph}(\lambda) d\lambda}. \quad (14)$$

The summary of the results concerning the  $\langle E_{ph} \rangle$  values is shown in **Figure 6b**. In particular, it demonstrates a shift of the emission spectrum of light sources towards shorter waves with an increase in the  $W_{ill}$  value, as illustrated in Figure 4b. Comparing the data in Figure 3, 5b, 6a, 6b, and Table 1, one can conclude that the light-induced dissociation of FeB pairs becomes more pronounced with rising average photon energy. Specifically, the constant  $K$  and the dissociation rate  $R_d$  increase and, therefore, the illumination time necessary for a complete complex decay decreases. Hence, for the dissociation of FeB pairs, the energy expended during the thermalization of non-equilibrium carriers also holds significance. The obtained results offer some conclusions about the mechanism of FeB dissociation. As discussed in the literature and previously mentioned, two possible ways of the second decay stage are typically considered: recharge of the iron ion and REDR. The latter arises from strong electron-lattice coupling at the defect site and involves utilizing local vibrational energy to promote pair dissociation [10, 5, 14]. The observed correlation between dissociation rate and photon energy in this study confirms the REDR process. Specifically, as photon energy increases, the production of non-equilibrium phonons during thermalization also rises. Furthermore, the increase in  $R_d$  value found in the experiment means an active in-

1 involvement of these quasi-particles in the dissociation of FeB pairs. Notably, recent research [5] focusing  
 2 on a detailed analysis of the dissociation and association reactions of the iron–boron pairs similarly con-  
 3 cluded the predominant role of REDR processes.  
 4

5

### 6 3 Conclusion 7

8

9 The effect of illumination spectra on the dissociation of FeB pairs in p–Si was investigated. We reported  
 10 the results of an experimental study of FeB dissociation rate in a solar cell based on Cz–Si, which was  
 11 carried out using different light sources and illumination intensities.  
 12

13

It was shown that the time required for the total dissociation of FeB pairs not only becomes shorter with  
 14 increasing the illumination intensity, but also significantly depends on a light source. As a result, the  
 15 determined value of material constant  $K$  varies within  $(1.5 - 3.8) \times 10^{-15}$  s for the used light sources.  
 16 The study of the illumination spectra allowed to conclude that the efficiency of FeB photo-dissociation  
 17 increases with the photon energy. This, in turn, indicates that the REDR effect is the dominant factor  
 18 during the second stage of light-induced dissociation of the FeB pairs. Furthermore, the obtained results  
 19 could help to develop defect engineering procedures for effectively converting unintentional iron impuri-  
 20 ties in silicon into high-mobility states, which could significantly impact semiconductor technology.  
 21

22

23

### 24 4 Experimental Section 25

26

27 The  $n^+$ - $p$ - $p^+$ -Si samples were used in the experiment. The structure was fabricated from a  $380\text{ }\mu\text{m}$  thick  
 28  $p$ -type boron-doped Czochralski silicon (100) wafer with hole concentration  $p = 1.36 \times 10^{15}\text{ cm}^{-3}$ . The  $n^+$   
 29 emitter with a sheet resistance of about  $20 - 30\text{ }\Omega/\square$  and thickness of  $0.7\text{ }\mu\text{m}$  was formed by phosphorus  
 30 diffusion. The anti-recombination isotype barrier was created by using a  $p^+$  layer ( $10 - 20\text{ }\Omega/\square$ ,  $0.6\text{ }\mu\text{m}$ )  
 31 formed by boron diffusion. On the front surface,  $\text{SiO}_2$  (40 nm) and  $\text{Si}_3\text{N}_4$  (30 nm) films were formed as  
 32 antireflective and passivating layers, respectively. The solid and grid Al contacts were formed by mag-  
 33 netron sputtering on the back and front surfaces, respectively.  
 34

35

A sufficiently high concentration of iron in the examined samples resulted from using impure chemicals  
 36 during the chemical treatments in the technological process. This production flaw, which was subsequently  
 37 corrected, allowed for the creation of model samples to study the effects associated with iron–boron pairs  
 38 in silicon solar cells. Details regarding the iron contamination in the sample are described elsewhere [21].  
 39 The area of the samples used in the study was  $1 \times 1\text{ cm}^2$ . The entire surface of the solar cell was illuminated  
 40 during the experiments.

41

43 Three powerful halogen lamps from different manufacturers were used for sample illumination and were  
 44 employed for the light-induced dissociation of FeB pairs:  
 45

46

- Orion Haltlichtspiegel 52240.0, 24 V, 200 W (labeled as “Orion” in the paper);
- Osram 64653 HLX ELC, 24 V, 250 W (Osram);
- General Electric 43537 H271, 20 V, 150 W (GE);

50

51

The light sources were powered by the DC Power Supply ITECH IT6332B, which allowed the current to  
be set through the lamp with an accuracy of 1 mA.

52

53

The illumination was transmitted from the sources to the sample via a fiber. The source emission at the  
 54 fiber output underwent a calibration using an optical power and energy meter Thorlabs PM100D and a  
 55 high-resolution sensor S401C, thereby enabling a direct assessment of the light flux incident on the sam-  
 56 ple. The illumination spectra at the fiber output were recorded using a spectrometer IKC-6 with a ger-  
 57 manium photodiode with calibrated spectral sensitivity.

58

59

The current-voltage characteristics were measured using a Keithley 2450 source meter and low-intensity  
 60 monochromatic light source (light-emitting diode SN-HPIR940nm-1W with light wavelength 940 nm  
 61 and intensity of about  $400\text{ }\mu\text{W}$ ). The LED radiation intensity was stabilized by a W1209 thermostat and  
 62 a power supply regulated by a circuit incorporating positive feedback and digital control.  
 63

64

65

1 The measurements were carried out at the temperature of 340 K. The sample temperature was driven  
2 by a thermoelectric cooler controlled by an STS-21 sensor and maintained constant [by](#) a PID algorithm  
3 embedded in the software that serves the experimental setup.  
4

## 5 Supporting Information

6 Supporting Information is available from the Wiley Online Library or from the author.  
7

## 8 Acknowledgements

9 The authors are grateful [to Prof. Vitaliy Kostylyov for his help in](#) calculating the reflectance [of](#) solar  
10 cells.  
11

## 12 Conflict of Interest

13 The authors declare no conflict of interest.  
14

## 15 Data Availability Statement

16 The data that support the findings of this study are available from the corresponding author upon rea-  
17 sonable request.  
18

19

20

## 21 References

22 [1] X. Cai, S.-H. Wei, *J. Appl. Phys.* **2023**, *134*, 22 220901.  
23

24 [2] J. Vobecky, *Phys. Status Solidi A* **2021**, *218*, 23 2100169.  
25

26 [3] J. Frascaroli, P. Monge Roffarello, I. Mica, *Phys. Status Solidi A* **2021**, *218*, 23 2100206.  
27

28 [4] M. K. Juhl, F. D. Heinz, G. Coletti, D. Macdonald, F. E. Rougiew, F. Schindle, T. Niewelt, M. C.  
29 Schubert, In *2018 IEEE 7th World Conference on Photovoltaic Energy Conversion (WCPEC) (A*  
30 *Joint Conference of 45th IEEE PVSC, 28th PVSEC & 34th EU PVSEC)*. **2018** 0328–0332.  
31

32 [5] C. Sun, Y. Zhu, M. Juhl, W. Yang, F. Rougiew, Z. Hameiri, D. Macdonald, *Phys. Status Solidi*  
33 *RRL* **2021**, *15*, 12 2000520.  
34

35 [6] E. Weber, *Appl. Phys. A* **1983**, *30*, 1 1.  
36

37 [7] H. Nakashima, T. Sadoh, T. Tsurushima, *Phys. Rev. B* **1994**, *49*, 24 16983.  
38

39 [8] F. E. Rougiew, C. Sun, D. Macdonald, *Sol. Energy Mater. Sol. Cells* **2018**, *187* 263 .  
40

41 [9] L. Ning, L. Song, J. Zhang, *J. Alloys Compd.* **2022**, *912* 165120.  
42

43 [10] C. Möller, T. Bartel, F. Gibaja, K. Lauer, *J. Appl. Phys.* **2014**, *116*, 2 024503.  
44

45 [11] L. J. Geerligs, D. Macdonald, *Appl. Phys. Lett.* **2004**, *85*, 22 5227.  
46

47 [12] N. Khelifati, H. S. Laine, V. Vähänissi, H. Savin, F. Z. Bouamama, D. Bouhafs, *Phys Status Solidi*  
48 *A* **2019**, *216*, 17 1900253.  
49

50 [13] S. Herlufsen, D. Macdonald, K. Bothe, J. Schmidt, *physica status solidi (RRL) – Rapid Research*  
51 *Letters* **2012**, *6*, 1 1.  
52

53 [14] D. H. Macdonald, L. J. Geerligs, A. Azzizi, *J. Appl. Phys.* **2004**, *95*, 3 1021.  
54

55 [15] L. Kimerling, J. Benton, *Physica B+C* **1983**, *116*, 1 297.  
56

57 [16] X. Zhu, D. Yang, X. Yu, J. He, Y. Wu, J. Vanhellemont, D. Que, *AIP Adv.* **2013**, *3*, 8 082124.  
58

59 [17] X. Zhu, X. Yu, P. Chen, Y. Liu, J. Vanhellemont, D. Yang, *Int. J. Photoenergy* **2015**, *2015* 154574.  
60

61 [18] T. T. Le, Z. Zhou, A. Chen, Z. Yang, F. Rougiew, D. Macdonald, A. Liu, *J. Appl. Phys.* **2024**,  
62 *135*, 13 133107.  
63

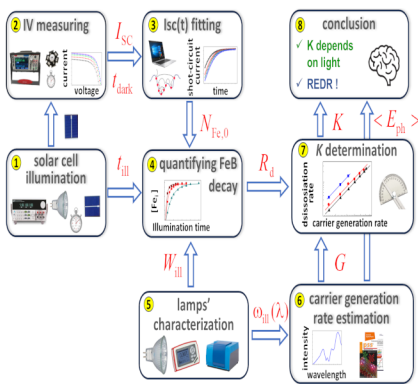
64

65

- 1 [19] K. Lauer, C. Möller, D. Debbih, M. Auge, D. Schulze, In *Gettering and Defect Engineering in Semi-*  
2 *conductor Technology XVI*, volume 242 of *Solid State Phenomena*. Trans Tech Publications Ltd,  
3 **2016** 230–235.
- 4
- 5 [20] W. Wijaranakula, *J. Electrochem. Soc.* **1993**, *140*, 1 275.
- 6
- 7 [21] O. Olikh, V. Kostylyov, V. Vlasiuk, R. Korkishko, Y. Olikh, R. Chupryna, *J. Appl. Phys.* **2021**,  
8 *130*, 23 235703.
- 9
- 10 [22] J. D. Murphy, K. Bothe, M. Olmo, V. V. Voronkov, R. J. Falster, *J. Appl. Phys.* **2011**, *110*, 5  
11 053713.
- 12
- 13 [23] O. Olikh, V. Kostylyov, V. Vlasiuk, R. Korkishko, R. Chupryna, *J. Mater. Sci.: Mater. Electron.*  
14 **2022**, *33*, 16 13133.
- 15
- 16 [24] J. Tan, D. Macdonald, F. Rougier, A. Cuevas, *Semicond Sci. Technol.* **2011**, *26*, 5 055019.
- 17
- 18 [25] D. Macdonald, A. Cuevas, L. J. Geerligs, *Appl. Phys. Lett.* **2008**, *92*, 20 202119.
- 19
- 20 [26] D. Klaassen, *Solid-State Electron.* **1992**, *35*, 7 953.
- 21
- 22 [27] T. Niewelt, B. Steinhauser, A. Richter, B. Veith-Wolf, A. Fell, B. Hammann, N. Grant, L. Black,  
23 J. Tan, A. Youssef, J. Murphy, J. Schmidt, M. Schubert, S. Glunz, *Sol. Energ. Mat. Sol.* **2022**, *235*  
24 111467.
- 25
- 26 [28] L. E. Black, D. H. Macdonald, *Sol. Energ. Mat. Sol.* **2022**, *234* 111428.
- 27
- 28 [29] M. Libra, V. Poulek, P. Kourim, *Research in Agricultural Engineering* **2017**, *63*, 1 10.
- 29
- 30 [30] R. Pässler, *Phys. Rev. B* **2002**, *66* 085201.
- 31
- 32 [31] N. Klyui, V. Kostylyov, A. Rozhin, V. Gorbulik, V. Litovchenko, M. Voronkin, N. Zaika, *Opto-*  
33 *Electr. Rev.* **2000**, *8*, 4 402.
- 34
- 35 [32] S. Schäfer, R. Brendel, *IEEE J. Photovolt.* **2018**, *8*, 4 1156.
- 36
- 37 [33] M. A. Green, *Prog. Photovoltaics Res. Appl.* **2022**, *30*, 2 164.
- 38
- 39 [34] S. C. Baker-Finch, K. R. McIntosh, D. Yan, K. C. Fong, T. C. Kho, *J. Appl. Phys.* **2014**, *116*, 6  
40 063106.
- 41
- 42 [35] S. Bowden, R. A. Sinton, *J. Appl. Phys.* **2007**, *102*, 12 124501.
- 43
- 44 [36] J. Lagowski, P. Edelman, A. M. Kontkiewicz, O. Milic, W. Henley, M. Dexter, L. Jastrzebski, A. M.  
45 Hoff, *Appl. Phys. Lett.* **1993**, *63*, 22 3043.
- 46
- 47
- 48
- 49
- 50
- 51
- 52
- 53
- 54
- 55
- 56
- 57
- 58
- 59
- 60
- 61
- 62
- 63
- 64
- 65

1  
2  
3  
4  
5  
6  
7  
8  
9  
10  
11  
12  
13  
14  
15  
16  
17  
18  
19  
20  
21  
22

## 23 Table of Contents



38 The results of a study on the kinetics of FeB pair dissociation in Cz–Si:B using different light sources are reported. The  
 39 dissociation rate was shown to depend not only on the intensity but also on the illumination spectrum. The investiga-  
 40 tion revealed an increase in dissociation efficiency with a decrease in wavelength and highlighted the dominant role of the  
 41 recombination-enhanced defect reaction.

42  
43  
44  
45  
46  
47  
48  
49  
50  
51  
52  
53  
54  
55  
56  
57  
58  
59  
60  
61  
62  
63  
64  
65



Click here to access/download  
**Supporting Information**  
SupportingInformation.pdf



Click here to access/download  
**Production Data**  
Fig3d.PNG



Click here to access/download  
**Production Data**  
Fig4a.PNG



Click here to access/download  
**Production Data**  
Fig4b.PNG



Click here to access/download  
**Production Data**  
Fig5a.PNG



Click here to access/download  
**Production Data**  
Fig5b.PNG



Click here to access/download  
**Production Data**  
Fig6a.PNG





Click here to access/download  
**Production Data**  
Fig6b.PNG



Click here to access/download  
**Production Data**  
manuscriptR.tex



Click here to access/download  
**Production Data**  
MSP.bst



Click here to access/download  
**Production Data**  
olikh.bib



Click here to access/download  
**Production Data**  
WileyMSP-template.cls





Click here to access/download  
**Production Data**  
Fig1.png



Click here to access/download  
**Production Data**  
Fig2a.PNG



Click here to access/download  
**Production Data**  
Fig2b.PNG



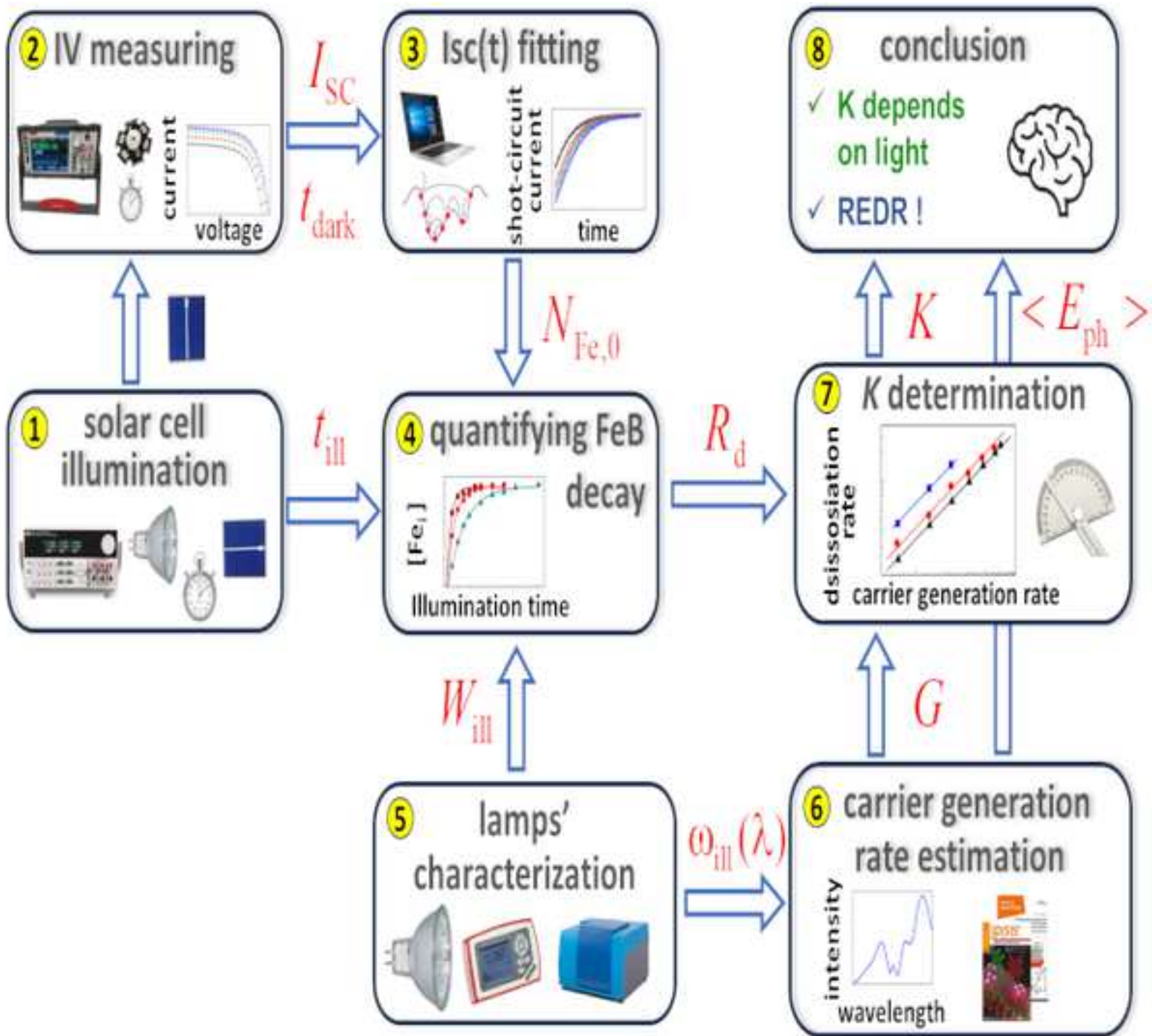
Click here to access/download  
**Production Data**  
Fig3a.PNG



Click here to access/download  
**Production Data**  
Fig3b.PNG



Click here to access/download  
**Production Data**  
Fig3c.PNG





The results of a study on the kinetics of FeB pair dissociation in Cz-Si:B using different light sources are reported. The dissociation rate is shown to depend not only on the intensity but also on the illumination spectrum. The investigation reveals an increase in dissociation efficiency with a decrease in wavelength and the dominant role of the recombination-enhanced defect reaction.